Fermilab Proposal No. 490

Scientific Spokesman:
J. Sandweiss
Yale University
(203) 436-1581

SEARCH FOR SHORT LIVED PARTICLES USING A HIGH RESOLUTION STREAMER CHAMBER

M. Dine, D. Ljung, T. Ludlam, R. Majka, J. Marx,
P. Nemethy. J. Sandweiss, A. Schiz, J. Slaughter, H. Taft

Yale University, New Haven, Connecticut 06520

M. Atac, S. Ecklund

Fermi National Accelerator Laboratory, Batavia, Illinois 60510

MAY 1976

I. INTRODUCTION AND OVERVIEW

The relatively old hypothesis[1] that there exists an as yet undiscovered family of hadrons, characterized by a new quantum number, has recieved substantial but still indirect support by the discovery of the J/ψ [2] states at SPEAR and BNL, and the observation of di-leptons[3, 4] produced in high energy neutrino interactions. A theoretical framework which interprets these results in terms of the "charm" hypothesis has been developed.[5] Although the details may well be incorrect, certain important features follow generally from the idea that the above phenomena are related to a new quantum number which is conserved in strong interactions and violated in weak interactions. Thus one expects that mesons exist which carry the new quantum number and which decay by the weak interaction. The mass of these mesons, if they exist, would have to be ~ 2 GeV/c^2 and their lifetime is reasonably estimated to lie in the range $10^{-(13 \pm 1)}$ seconds. In the following, without prejudice towards the ultimate correctness of the charm scheme, we shall refer to such new short lived particles as "D" particles.

A variety of experiments have been carried out and/or are in progress at SPEAR, and with photon and hadron beams at FNAL and BNL to search for the new particles by looking for narrow (resolution limited) peaks in various effective mass spectra. These experiments have the drawback that their significance depends on an unknown branching ratio for decay into the particular exclusive channels which are studied. Because of spectrometer acceptance they are also, to varying degrees, sensitive to the unknown production dynamics of the new particles. At the time of writing no positive results have been reported.

Clearly, direct visual observation of the production and subsequent decay of a "D" particle would be of great value in providing direct evidence for a new particle which decays via the weak interaction. A rough estimate of the required detector resolution is obtained by calculating the mean laboratory decay distance $\bar{\ell}$ of a centrally produced ($X_{Feynman} = 0$) D particle in ~ 200 GeV $\pi^- p$ collisions.

$$\bar{\ell} \sim \gamma_{CM} \cdot 3 \times 10^{10} \times 10^{-13} \text{ cm}$$

$$\therefore \bar{\ell} \sim .3 \text{ mm}$$

Thus, resolutions small compared to 300μ are required. A more careful analysis (Cf. Section III-C) shows that $\sim 10\mu$ resolution in a visual detector would allow useful efficiencies for detection of D particles with lifetimes as small as $\sim 2 \times 10^{-14}$ seconds.

Until recently, only the nuclear emulsion technique provided a visual detector with resolution of this order. Indeed, nuclear emulsions are readily capable of $\leq 1\mu$ resolution and could observe lifetimes of $\sim 10^{-15}$ second. However, nuclear emulsions suffer from two serious drawbacks. First, they are continuously sensitive and they integrate tracks from all incident particles from the time the emulsions are manufactured until the time they are developed. Second, they have a relatively high density (3.81 gms/cm^3) and short radiation length (2.94 cm), so that secondary interactions of hadrons and photons occur frequently and form a background which constitutes a "noise level" which must be exceeded by D particle decays for a significant observation to be made.

In order to utilize the benefits of a visual, triggerable, low density detector for new particle searches, we have designed and are constructing a small, high pressure streamer chamber which should produce streamers of 25-50μ diameter, and resolutions, in space, of $\leq 10\mu$. The details of the design and of the current state of the chamber construction and test program are given in Appendix I. The chamber will be completed early this summer. After initial tests with cosmic rays at Yale, we plan to move the chamber to the test beam at FNAL to complete the tests of resolution and to optimize the chamber operating parameters.

It seems very reasonable to us to estimate the completion of the chamber test and optimization program to occur in late Fall 1976. Because of the very topical character of the search for new particles we would very much like to move the chamber into an experimental setup as soon thereafter as possible.

If we could begin running in the Winter of 76-77, we believe we could have significant results (approximately 1/2 the data sample) by Mid-Summer 1977. In considering the reality of this time scale, it is important to note that this experiment, although it contains certain unusual technical components, is rather small by high energy physics standards as regards both physical size and complexity. For example, exclusive of the accelerator and beam line, the entire experiment occupies a floor space of less than 2 m x 2 m.

We realize that it is unusual (although not unprecedented) to submit a proposal to perform an experiment with a new instrument before it has been experimentally tested. Naturally, any approval of the experiment would be conditional upon the verification of the chamber design performance. We seek such conditional approval because it would greatly facilitate the rapid transition from test program to experiment. We also believe as is detailed in Appendix I that there is very little risk of not meeting the design specifications as the scaling principle upon which the chamber design is based is both well tested and well understood in gas discharge physics.

In the experiment we propose, we plan to trigger the chamber on interactions of high energy π^- ($\sim$ 200 GeV), in the chamber gas, which produce a "muon" within a range of 30 to 300 mr and with energy greater than 2.3 GeV. This scheme is based on the belief that any weak decay interaction is likely to produce substantial semileptonic decays ($D \rightarrow \mu + x$). Studies of the muon trigger systematics, which use actual high energy inclusive data, show that the false muon rate from ordinary events is $\sim .4\ ^{o}/o$ per event.

We request 800 hours of data taking time in a 200 GeV/c π^- beam of intensity 8×10^5 per pulse and with a spot size of 5 mm by 1 mm. The details of expected event rates and backgrounds are presented in a subsequent section, but we list here the major physics goals of the experiment.

(1) Search for new short lived particles produced in hadronic collisions

(a) in a manner independent of decay mode

(b) with $\sim 4\pi$ geometry and hence with a sensitivity which is independent (see also Section III-C) of production dynamics

(c) with a resulting sensitivity such that production cross sections comparable to those for ψ/J production would be successfully detected.

(2) If such particles exist, our technique would allow

(a) direct measurement of the lifetime and thus prima facie evidence for the weak decay interaction

(b) direct observation of whether or not the new particles are pair produced (as they should be if they carry a new quantum number)

(c) observation of charged particle decay multiplicities for the new particles

(d) a preliminary measurement of their semi-leptonic branching ratio

(e) measurement of total production cross sections for the new particles

(f) observation of the topological and kinematical character of the events in which the new particles are produced (and as a corollary, learn how to improve our triggers)

(g) search for new "short time" phenomena associated with the new particles (e.g., D → heavy lepton)

(h) the development of future experiments using the high resolution streamer chamber in a more complex hybrid system.

(2) (h) - cont'd.

For example, one could imagine a downstream effective mass spectrometer which uses the streamer chamber pictures to identify the D particle decay tracks to eliminate combinatorial and related backgrounds in effective mass studies. Such a hybrid system might be a very powerful tool for exploring the spectrum of higher mass states carrying the new quantum number, which can decay strongly.

II. APPARATUS AND EXPERIMENTAL METHOD

A. Experiment Design

The layout of the experiment is shown in Fig. 1. The scintillation counters S1, S2, VH1 ("hole" veto) define the incident beam to lie within a transverse region of 1 mm x 5 mm. The corresponding areas in the pressure windows are .001" stainless steel foils. The interaction hodoscope H is used to signature interactions in the gas (or the pressure windows). The scintillation counter S3 is used to detect particles which penetrate the muon filter and the chambers P1, P2 provide position (to within $\sim$ 0.5 cm) and direction (to within $\sim$ $.3^{o}$) information on the particles which penetrate the filter. The chambers P1, P2 can be either multiwire proportional chambers (with $\sim$ 1 cm wire spacing) or drift chambers. The data from P1 and P2 are not used in the trigger but are recorded for each event. As will be discussed in Section III-D, this information will be very useful in reducing strange particle and secondary interaction background events which can simulate D particle decays.

The trigger requirement will be:

$$S1 \cdot S2 \cdot \overline{VH1} \cdot (H \geq 2) \cdot S3$$

which will initiate the high voltage pulse to the chamber.

The resulting pictures will be of two types. One, in which the trigger interaction occurred in the 3.5 cm fiducial length and another in which the trigger interaction occurred before or after this fiducial region. The latter will be readily eliminated in the scanning. The former, which will comprise 24 ^{o}/o of the total, will be carefully scanned for tracks which do not have a common origin. Computer simulated pictures have been generated and test scanned (see, Section III-C) and we have found that searching for tracks which "miss the vertex" is a rapid and efficient scanning procedure for detecting short lived decays. We note that since there is no magnetic field, all tracks are

straight. Once an event has been "flagged" in scanning, it will be very carefully measured and constrained fits made to determine the production and decay vertices with maximum accuracy.

B. Chamber and Optics

Figure 2 shows the chamber assembly in its pressure vessel. The entire assembly is essentially one 27 Ω parallel plate transmission line with a Blumlein pulser on one end, a matched terminator on the other end, and the chamber gap in the middle.

Appendix I gives a detailed discussion of the chamber design and construction and we recapitulate here the salient points for the experiment. The central Blumlein electrode (5 cm long) is charged via a small spark gap from a relatively standard 10 stage Marx generator ($V_{out} \leq$ 400 KV Max, t_{rise} = 25 ns). The Blumlein central electrode is shorted to the bottom (ground) electrode by the action of four spark gaps which will be preloaded with photo-electrons liberated from the stainless steel cathodes by ultra-violet light from the charging gap. There should be negligible jitter in the action of the spark gaps and the resulting pulse to the streamer chamber gap should have a rise time of $\leq$ 100 pico seconds, a width of .4 ns (FWHM), and amplitude up to 200 KV.

The visible chamber gap is 0.5 cm high and 4 x 4 cm transverse. The gap is photographed from each side by an F16 (20 atmospheres) to F8 (40 atmospheres) lens with demagnification of 1.5. The transparent electrodes are made of 12μ Tungsten wires spaced every 100μ. The lenses are borrowed from the Yale PEPR system and the entire optical system including the "transparent" wire electrode has been set up and tested successfully. The depth of focus is 2.5 mm at F16 and 50μ diameter streamers will have apparent signs varying between 55μ and 65μ. At F8, 25μ diameter streamers will appear as 27.5μ to 32.5μ over a 1.25 mm deep field of view. As noted in Appendix I, we expect the diffusion of the primary electrons before application of the high voltage to give rise to a streamer r.m.s. scatter about the "true position" of 10μ.

The cameras are borrowed from Brookhaven National Laboratory where they had been used for the 30'' hydrogen bubble chamber. They take 35 mm, sprocketed film and are equipped with vacuum platens and easily match the film flatness and mechanical stability requirements for the streamer chamber. The camera advance deadtime is 100 ms.

C. The Muon Trigger

As noted above, the trigger requirement includes the detection of one (or more) particles which penetrate the heavymet hadron filter. The main properties of the hadron filter are listed below.

Material	Heavymet or equivalent (sintered Tungsten)
Density	18.0 gms/cm^3
Absorption mean free path for pions	13.0 cm (234 gms/cm^2)
Length	110 cm
Angular range subtended (from center of chamber)	30 mr to 300 mr
Minimum Muon Energy required to penetrate filter	2310 MeV

The pion mean free path (for inelastic collisions) was estimated as follows. Crannell, et al.[6] have measured the absorption mean free path of pions and protons in iron at energies of 9 to 18 GeV and have found

$$\lambda_\pi = 1.18 \ \lambda_p$$

We have assumed the same ratio applies for Tungsten and using λ_p = 134 gms/cm^2 [6, 7] for the absorption mean free path for protons in iron and assuming that λ(gms/cm^2) is proportional to $A^{1/3}$, we obtain the value λ_π (Tungsten) = 234 gms/cm^2 listed in the table.

The expected efficiency of the muon trigger for D particle decays has been evaluated from a simple model of $D\bar{D}$ production as is explained in Section III-C. We discuss here our estimate of the fake rate, i.e., the probability that an ordinary interaction will produce a particle which counts in S3.

We begin with data from π^-p collisions at 150 GeV/c[8] which give us complete information on charged pions produced in inelastic collisions. We assume that Feynman scaling applies and we compute the pion production spectra for 200 GeV/c incident momentum.

Thus we find that, on the average, 2.5 pions (including π^+ and π^-) impinge on the filter per inelastic collision in the chamber. These pions have momenta which extend from 2310 MeV to 75 GeV but are strongly peaked toward the low end. For example, the average energy (for pions above 2310 MeV) of pions which strike the filter is 11.1 GeV.

For each momentum of pion which strikes the filter we have considered the following seven sources of production of a particle which penetrates to S3.

P_1 : The probability of the pion decaying into a muon (of sufficient energy) before striking the shield.

P_2 : The probability of decaying into a muon of sufficient energy before the first interaction.

P_3 : The probability of the pion penetrating the shield without an inelastic interaction.

P_4 : The probability of pions produced by the first inelastic interaction decaying into penetrating muons before they interact again in the shield.

P_5 : The probability that pions produced by the first inelastic interaction will penetrate the shield without a subsequent inelastic interaction.

P_6 : The probability that pions produced in the second generation of inelastic collisions will decay into penetrating muons before they in turn interact again in the shield.

P_7 : The probability that pions produced in the second generation of inelastic interaction in the shield will penetrate the remainder of the shield without subsequent inelastic collision.

The inclusive spectra of pions produced in the shield was taken to be the same as those produced by π^+ p collisions for which good experimental data is available, and was used.[9] In these calculations the transverse spreading of the cascade was neglected which will cause us to slightly overestimate the fake rate. We have also neglected the contribution of penetrating particles from decay or punch through of the products of the third generation of collisions in the shield. This is justified because the average energy of the particles produced in succeeding generations of inelastic interactions drops rapidly and a negligible fraction of the pions produced in the third generation of inelastic collisions will have sufficient energy to penetrate the remainder of the shield.

The net probability,

$$\sum_{i=1}^{7} P_i \quad ,$$

was calculated for a number of incident pion energies and a smooth curve interpolated. This was then weighted with the energy spectrum of the pions from the interaction of the 200 GeV/c pions in the chamber and an average probability of "penetrating" the shield of 1.6×10^{-3} per pion incident obtained. Multiplying by the average number of pions striking the shield per event (2.5) we obtain a final fake rate of $.4 \times 10^{-2}$ per event.

A complete Monte Carlo simulation program which will include lateral spreading of the hadronic cascade is under preparation and will be used for final optimization of the parameters of the hadron filter.

III. EVENT RATES

A. Beam and Trigger Rates: 20 Atmosphere Chamber

Starting with a π^-p total cross section of 24 mb at 200 GeV/c,[10] subtracting an elastic contribution of 3.3 mb[11] and assuming an $A^{2/3}$ dependence of the cross section, we obtain the average inelastic cross section of π^- on our Neon-Helium mixture,

$$\sigma \text{ (INTERACTION)} = 143 \text{ mb.}$$

At a pressure of 20 atmospheres, the 12.0 cm depth of the chamber then gives an interaction probability, per incident pion, of $P_{NeHe} = 9.2 \times 10^{-4}$. We add a probability $P_W = 2 \times 10^{-4}$ for interactions in the stainless steel pressure windows (of 0.001" each) to obtain a total interaction probability of

$$P \text{ (INTERACTION)} = 11.2 \times 10^{-4}/\text{Pion.}$$

The fraction of interactions in our 3.5 cm deep fiducial volume is F(fiducial) = 24 %.

In addition to an interaction signature (which we assume to be 100 % efficient), we require each event to give a signal in the muon detector, where the rate of false triggers/interaction is μ(false) = 0.40 % (see Section II-C). Our trigger rate per incident pion is thus P(interaction) x μ(false), or

$$R \text{ (trigger)} = 4.48 \times 10^{-6}/\pi^-.$$

With a pion beam of 8×10^5/spill, we get an event rate of 3.6 events/spill. A 100 ms camera deadtime reduces this rate to 2.4 events/spill. In 800 hours of running, at 1 spill/10 seconds, we therefore collect

$$N \text{ (pictures)} = 6.8 \times 10^5$$

on film. We get the number of pictures with an interaction in the fiducial volume

by multiplying this number by F(fiducial):

$$N \text{ (fiducial)} = 1.6 \times 10^5 .$$

B. Charmed Events

If we let B_μ be the branching ratio $D \to \mu \nu x / D \to \text{All}$, and let σ_D be the production cross section of charmed pairs on nucleons, $\pi^- p \to D\bar{D}X$, and if we assume that this cross section also varies as $A^{2/3}$, then the fraction of our pictures with $D\bar{D}$ pairs is

$$F(D\bar{D}) = \frac{\sigma_D}{\sigma_{\pi^- p} \quad \mu \text{ (false)}} \times \epsilon_\mu B_\mu (2 - \epsilon_\mu B_\mu) ,$$

where $\sigma_{\pi^- p}$ is the inelastic π^- cross section on protons, and ϵ_μ is the detection efficiency of our muon detector for muons from D-decay. Using Monte Carlo events of D production and decay (described in detail in Section III-C, following), together with the muon detector geometry (from Section I-D), we estimate $\epsilon_\mu = 65\ ^o/o$. We therefore have

$$F(D\bar{D}) = .016\ \sigma_D\ (\mu b)\ B_\mu\ (1 - 0.3\ B_\mu) .$$

The total number of $D\bar{D}$ decays in our 1.6×10^5 fiducial pictures will therefore be

$$N(D\bar{D}) = 2620\ \sigma_D\ (\mu b)\ B_\mu\ (1 - 0.3\ B_\mu) .$$

For a branching ratio of $B_\mu = 10\ ^o/o$ the total number on film is $N(D\bar{D}) / \sigma_D = 280$ events/μb.

C. Scanning Efficiency

In order to get an estimate of our efficiency for the detection of D-particle pairs on film, we have generated "charmed events" by a Monte Carlo simulation of the experiment.

We have assumed the associated production of $D\bar{D}$, a D mass of 2.2 GeV/c^2, and a decay mode $D \rightarrow K\pi\pi\pi$ . . . with a mean decay product multiplicity of 3.6 particles/D. We have assumed that the decay products are distributed uniformly in phase space and that 2/3 of the pions and 1/2 of the kaons are charged. We assumed further that the D particles are produced centrally, with a Gaussian rapidity distribution of

$$\frac{d\sigma}{dy} = e^{-2y^2}$$

and a transverse momentum distribution of $e^{-1.5\ p_T^2}$. Finally, we superimposed these $D\bar{D}$ decays on actual events from a 150 GeV/c π^- bubble chamber exposure[8] from which we threw away pion tracks until the visible energy of the total event was consistent with energy conservation. The mean visible track multiplicity of the resulting composite events was 8.5.

For 53 such Monte Carlo events we generated computer plotted "photographs" of streamer chamber events, with 55 micron apparent streamer size, 10 micron diffusion, and a statistical distribution of streamers with a mean density of 20/cm. A double scan of these pictures gave 30/53 = 57 ^{o}/o detected events, 62/252 = 25 ^{o}/o detected D decay tracks and a scanning inefficiency of about 5 ^{o}/o. Figures 3 and 4 show one of our "detected" computer photographs, first raw, then interpreted.

From these 53 pictures we developed a one-parameter algorithm for the detection efficiency of a given D-decay product, then applied this algorithm to a variety of 500 event Monte Carlo samples. The detection efficiency is a strong function of the proper lifetime, t_o, of the D-particles, but turns out to be singularly insensitive to our other assumptions. In particular, we observe no significant change of the efficiency vs. lifetime above $\epsilon(t_o)$ when we switch from central to an extreme peripheral model of D-production, when we change the incident beam momentum from 150 GeV/c to 250 GeV/c, or when we change D-decays to a semi-leptonic mode. Figure 5 shows $\epsilon(t_o)$ for central and for peripheral D-production models. We see that the efficiency exceeds 10 ^{o}/o

down to a lifetime $t_o = 2 \times 10^{-14}$ sec, and crosses 50 °/o at $t_o \sim 10^{-13}$ sec.

The detected number of $D\bar{D}$ decays will be N $(D\bar{D})$ x $\epsilon(t_o)$, or

$$N\ (DET) = 2620\ \sigma_D\ (\mu b)\ B_\mu\ (1 - 0.3\ B_\mu)\ \epsilon(t_o) \ .$$

If we also require that the muon track which triggers our event be one of the detected D decay products (a powerful cut against backgrounds, see next Section), we find that the scanning efficiency drops by about 40 °/o in the entire lifetime range we are considering. The detected number of events becomes

$$N\ (DET) = 1570\ \sigma_D\ (\mu b)\ B_\mu\ (1 - 0.3\ B_\mu)\ \epsilon(t_o) \ .$$

For $B_\mu = 10$ °/o and $t_o = 10^{-13}$ sec we get

$$N\ (DET) / \sigma_D = 88 \text{ events}/\mu b \ .$$

It is of interest to ask whether we can see both D and $\bar{D}$ on a given picture and thus prove that we do indeed have associated pair production. Two tracks which do not come from the original vertex and are also incompatible with a common secondary vertex signal associated production.

Of our sample of 53 simulated events we find that there are 7 events that we can identify as $D\bar{D}$. We give a rough estimate of the $D\bar{D}$ double detection efficiency vs. lifetime in the table below:

t_o	$\epsilon_2(t_o)$
5×10^{-13}	30 °/o
2.5×10^{-13}	15 °/o
1.0×10^{-13}	10 °/o
5×10^{-14}	2 °/o

Again, for $B_\mu = 10^{0}/o$, $t_o = 10^{-13}$, we get

N (detected associated prod) = 25 eV/μb .

D. Backgrounds

A D-vertex in our events could be simulated by (1) a mismeasured track from the main vertex; (2) external e^+e^- pairs from π^o decay; (3) secondary interactions of hadrons from the original vertex; (4) strange particle decays.

(1) Measuring error. Our successful events in the Monte Carlo scanning experiment all had tracks which failed to fit the original vertex by 5 or more standard deviations. The odds against a track from the original vertex being out by 5 standard deviations are 1.7×10^6 to 1. We have an average multiplicity of 8 tracks[12] in our 1.6×10^5 pictures; thus we have ≤ 0.8 background events from mismeasured tracks.

(2) Electron pairs from π^o decay. Even though we expect to see 1700 externally converted pairs in our fiducial volume, they will all point back to the original vertex and thus will not contribute to the background.

(3) Secondary interactions. The mean potential path of secondary hadrons from the original vertex is 20 mm, the mean multiplicity is 8 (we assume that neutral tracks are dominated by π^o which do not contribute to interactions). From Section III-A the probability of interaction is 7.7×10^{-5} per cm of track so that our interaction probability per event is 1.2×10^{-3} and we have a total of 192 secondary interactions somewhere in the fiducial volume.

(4) Strange Particles. We start with the Λ^o and K^o production cross sections and momentum distributions of Bogert et al.[13] We find the mean potential path length in our fiducal volume and the decay probability along the potential path as a function of lab momentum, then average this probability over the momentum spectrum. We find that the probability of a Λ^o(or Σ^o) $\rightarrow \pi^- p$ decay in our fiducial volume is 2.4×10^{-3}/event and that of $K_s^o \rightarrow \pi^+\pi^-$ is 5.8×10^{-3}/event. For $\Sigma^\pm$ we assume that the production rates of Σ^o, Σ^+, Σ^-

are equal and that 1/3 of the observed Λ^o are in fact Σ^o. The total probability of charged Σ decay is then 1.6×10^{-3}/event. We multiply the sum of these probabilities (9.8×10^{-3}) by the number of our events (1.6×10^5) and predict 1570 strange decays somewhere in the fiducial region. The mean potential path for all these strange particles is 7.5 mm.

Secondary interactions and strange particle decays will both be distributed uniformly over their potential path. On the other hand, we do not look for D-s over this path length, but only over a region $\sim$1 mm long. Therefore, the fraction of background events competing with D-decay is $\sim$1 mm/potential path.[14]

The relevant background is therefore:

N (interactions) = 10 events;

N (strange particles) = 209 events.

The background is dominated by strange particle decays for which the muon trigger is "fake," hence uncorrelated with the decay products of the strange particle. On the other hand, the muon trigger for a $D\bar{D}$ event is "real;" the muon is one of the decay products. Thus, imposing the requirement that one of the D-decay candidates should correspond to a muon track in the muon detector (this requirement reduces our efficiency for $D\bar{D}$ detection by $\sim$40 %) cuts the strange particle background drastically. In fact, the only limits to the rejection power are the multiple scattering of the muon in the muon detector and the small angle stereo reconstruction of the dip angle which limit our muon track line-up accuracy to about 1^o. With this resolution we find that we have a rejection factor of 60 against strange particles and $\sim$ 30 against interaction backgrounds.

The final background levels are therefore

N (mismeasurement) = 0.8 event,

N (interactions) = 0.3 event,

N (strange particles) = 3.5 events,

for a total of 4.6 background events.

E. Cross Section Limits

If the D production cross section corresponds to an expected number of 12 events, with a background of 5 events, the expected number of events is 17 ± 4.1. The observed number of events is then greater than 10.3 with 95 °/o probability. In turn, the odds against a 10.3 event result in the absence of a charmed signal (a 3 standard deviation fluctuation from 4.1 background events) is greater than 99 to 1. Hence a 12 event signal level corresponds to a very confident claim for D production.

In the following Table we list the cross sections needed for a 12 event signal, for several D lifetimes.

t_o(sec)	$\sigma_D B_\mu$	σ_D for B_μ = 10 °/o
5×10^{-13}	8 nb	80 nb
2×10^{-13}	9 nb	90 nb
10^{-13}	12 nb	120 nb
5×10^{-14}	20 nb	200 nb
2×10^{-14}	50 nb	530 nb

F. Operation at 40 Atmospheres

If we are able to increase the operating pressure of the chamber from 20 to 40 atmospheres, the rate of inelastic interactions doubles, but the trigger rate goes up by only 50 °/o because of the increased camera deadtime. In 800 hours of data taking we then obtain 2.4×10^5 fiducial pictures. The secondary interaction background per event doubles, but this increases the total background per event by only 10 °/o.

The main effect of changing the pressure is again seen from the scaling principle: we expect increased streamer density and half the streamer size. If we are able, by judicious "poisoning" to reduce the diffusion to match, then we have a device of twice the resolution. This improvement translates directly to a change of lifetime scale from t_o to $t_o/2$. Thus the scanning efficiency would drop to $10^o/o$ not at $2 \times 10^{-14^o}$ sec but at 1.0×10^{-14} sec. For short lifetimes this would be an important improvement.

IV. CONCLUSIONS AND SUMMARY

The advantages of a triggerable, high resolution, visual detector can be realized with the use of a small, high pressure streamer chamber of suitable design. We propose to use such a chamber, which is currently under construction at Yale, in an experiment at FNAL to search for and/or study new, short lived particles with lifetimes in the 10^{-13} second range.

We request a run of 800 hours in a 200 GeV π^- beam of intensity 8×10^5/spill which can be focussed to a 1 mm x 5 mm spot. The detection efficiency for $D\bar{D}$ events is $> 35\,^{o}/o$ for D lifetimes above $2.5 - 5.0 \times 10^{-14}$ sec, the precise limit depending on the detailed performance of the chamber. Production cross sections for $D\bar{D}$ events of 100 - 200 nb would result in a statistically and systematically significant observation of the new particles if their lifetimes were $\geq 2.5 - 5 \times 10^{-14}$ seconds. We note that the ψ / J production cross section in the forward hemisphere ($x > .05$) has been measured to be $\sim$ 74 nb for 150 GeV/c pions. If the backward production is comparable, the total 150 GeV/c π^- Nucleon ψ / J cross section would be $\sim$ 150 nb. In any case, we see that D production cross section comparable to ψ / J production cross sections would be successfully detected in our experiment.

The chamber will be completed in the summer of 1976 and will be moved to Fermilab for beam tests in the fall of 1976. We are requesting approval of our experiment now, conditional upon the successful operation of the chamber, in order to facilitate a rapid transition from test beam to experiment because of the very topical and fast moving character of this particular area of high energy physics.

APPENDIX I.

A. Scaling Principle and Chamber Parameters

The basic idea of the scaling principle for the chamber design is illustrated in Fig. 6. An electron, produced by an ionizing collision of the charged particle whose track is to be detected, is accelerated by the applied electric field and develops an avalanche which eventually grows into a photographable streamer. For any given avalanche such as the one with P_o, E_o, t_o we may consider a related scaled avalanche in which

$$p = sp_o$$

$$E = sE_o$$

$$t = t_o/s$$

Clearly, the average energy gain between collisions is the same in both scaled and unscaled avalanches and hence the two avalanches should have the same average development except that the statial dimensions of the scaled avalanche will be smaller by a factor S. The following table compares a "standard" streamer chamber with chambers scaled to 20 and 40 atmospheres.

Standard Chamber	Scaled: 20 Atmospheres	40 Atmospheres
Gas: Spark Chamber Neon (Ne-He 90/10)	.....Spark Chamber Neon	
Electric Field 10-20 KV/cm	200 - 400 KV/cm	400 - 800 KV/cm
Pulse Width (FWHM) 10-20 ns	.5 - 1 ns	.25 - .5 ns
Pulse Rise Time 2 -4 ns	.1 - .2 ns	.05 - .1 ns
Gap ~ 30 cm	.5 cm	.5 - .25 cm
Streamers/cm ~ 2.5	20 - 40	30 - 60
Streamer Diameter 1 mm	50 μ	25 μ

The underlined values are those chosen for the chamber under construction. We note that the number of streamers per cm does not scale simply as the pressure because of the inhibition of one streamer by the existence of a nearby streamer.

The one operating parameter which cannot be fully scaled is the time delay between the occurrence of the interesting event and the application of the high voltage pulse to the chamber. We will be able to apply the high voltage to the chamber 370 ns after passage of the beam particle. Typical standard chambers operate with ~1 μs delay, thus diffusion of the primary electrons prior to the application of the pulse will be relatively more serious in the high pressure chamber than in the standard chamber.

We estimate the effect of diffusion as follows. F. Villa[15] has analyzed the resolution obtained in a large number of streamer chamber experiments and has shown that the major contribution has come from film grain noise

(of $\sim 5\ \mu$). If we take the experiment with lowest demagnification (and best resolution) and ascribe all of the resolution width in excess of film grain noise to diffusion of the primary electrons, we would conclude that at atmospheric pressure $\sigma_{diff} = 100\ \mu$. Scaling to 20 atmospheres and 370 ns (instead of 800 ns), we would obtain[16] σ_{diff} (20 atmos.) = $15\ \mu$. If we take a more reasonable view that measurement error, optical distortions, etc. account for half the observed deviation, we would expect σ_{diff} (20 atmos.)= 7.5μ. In our scanning exercises we have taken $\sigma_{diff} = 10\ \mu$.

We comment that the diffusion is very sensitive to small admixtures of impurities in the gas. For example, the diffusion coefficient for pure Neon[17] is 7800 cm^2/sec, while commercial grade Neon has a diffusion coefficient of 790 cm^2/sec and Neon (1 atmosphere) with saturated C_2H_5OH vapor (room temperature) has a diffusion coefficient of 29 cm^2/sec. We thus feel confident that we will be able to find a suitable impurity gas to achieve the desired small diffusion. Indeed, as indicated above, simply using the standard spark chamber Neon as commercially supplied may suffice.

B. Spark Gaps and Blumlein System

In order to achieve the .5 ns width and .1 ns rise time of the high voltage pulse, the switch which shorts the central Blumlein electrode to the lower electrode of the transmission line must clearly operate in a comparable or shorter time. Figure 7 shows the design of our spark gap system. The spark gap end of the transmission line is enclosed in a Lexan housing which can withstand pressures up to 55 atmospheres.

A standard Marx generator (10 stage, $V_{out} \leq 400$ KV, $t_{rise} = 25$ ns) charges the small ($\sim$ 5 cm long(central Blumlein electrode through a small spark gap as shown in Fig. 7. The ultra-violet light from this charging spark liberates photo electrons from the stainless steel cathode surfaces. Calculations based on measurements of a spark gap triggered by an ultra-violet flash lamp[18] indicate that many thousands of electrons will be produced at each

gap. When the Blumlein electrode reaches the breakdown potential for the gaps, each gap should initiate breakdowns without the jitter associated with "waiting for the first electron in the gap." This design is based on the experience of the University of Washington group[19] who have designed and tested a similar system with 3 spark gaps illuminated by an axial gap charging the central electrode in a conical Blumlein system. The following table compares the operating parameters for the University of Washington system and the one proposed here.

University of Washington[19]	High Resolution Streamer Chamber
Output Voltage 180 KV	200 KV
Gap Spacing 20 mm	~ 3 mm (adjustable)
Pressure 11.2 atmospheres (absolute)	~ 50 atmospheres
Gas Argon	Argon
Risetime (Measured $\angle$ 0.4 ns	$\angle$ .1 ns (estimated)

We note that the limit of the risetime for the University of Washington pulser was due to the equipment used to measure the risetime, so that only an upper limit could be established. As is seen from the table, our spark gap design is roughly the same as theirs scaled by a factor of four.

Ideally, all points along the edge of the central electrode should short to ground at the same time. Calculations show, however, that four gaps are

adequate for the performance required. The entire electromagnetic design of the Blumlein system has been verified by the construction and testing of a 10 x scale model operated at low voltage (~100 Volts) with avalanche transistors replacing the spark gaps.

C. Chamber and Transmission Line

The output line of the Blumlein section is a 27 Ω parallel plate transmission line with 2.5 cm plate separation and polystyrene dielectric. These dimensions were chosen as a compromise between the desire to limit the propagation of non TEM modes and the desire to have sufficient spacing to withstand the high voltage pulse without breakdown. For the dimensions chosen, the cutoff frequency for the first higher mode is 4.0 Giga Hertz.

The entire system is a 27 Ω line. The transition region (cf. Fig. 2) in which the polystyrene dielectric is replaced by the chamber gas has the gap tapered so as to maintain the constant 27 Ω impedance. The resulting 1.6 cm gap is maintained through a section which contains cpacitative pick-off probes which will be used with a sampling scope system capable of 50 picosecond time resolution. In the interest of brevity, we do not discuss some of the interesting engineering aspects of this measurement system.

The transition to the 0.5 cm chamber gap is again at constant impedance as is the symmetric transition after the chamber to the matched terminator.

The terminator is a deliberately lossy section of line with the resistive loss and the taper of the gap chosen so as to maintain a constant 27 Ω impedance.[20] Not surprisingly, the total impedance of the lossy section to the short is 27 Ω . The lossy plate of the terminator is constructed by plating a ~ 1000 Å Nichrome coating on a plastic (CR - 39) substrate.

The chamber section is 10 cm long with 0.5 cm gap and 6 cm width, with plates of 1 cm thickness. The central 4 x 4 cm is "open" and 12 μ Tungsten wires with 100 μ spacing cross the open region to provide a pair of transparent electrodes.

D. Optics and Photography

The basic choice in the optical design is the trade-off between depth of field and diffraction. The apparent size (in space) of a streamer can be minimized for a given depth of field by equalizing the contributions from diffraction and displacement from the ideal object position. A depth of field of 1 - 2 mm is necessary to provide sufficient potential path for the observation of reaction products. The following table lists the parameters chosen.

	20 Atmospheres	40 Atmospheres
Demagnification	1.5	1.5
Numerical Aperture	F16	F8
Apparent Size (in space) of a 50 (25) μ streamer at center	55 μ	27.5 μ
Depth of Field of View	2.5 mm	1.25 mm
Apparent Size (in space) of a 50 (25) μ streamer at the edge of the field of view	65 μ	32.5 μ

We note that the number of photons per cm^2 on the film is greater (20 atmosphere chamber) than is the case for a standard chamber by a factor of $\sim$ 14. Finally, we note that the size of the streamer image on the film is $\sim$40 μ so that film grain noise ($\sim$5 μ) should make a negligible contribution to the chamber resolution. The lenses used are borrowed from the Yale PEPR system and were used in that system before its 5" CRT was replaced by a 9" CRT. The entire optical system including the "transparent" electrode has been set up and tested and the necessary resolution and depth of field has been obtained.

REFERENCES

1. B.J. Bjorken and S.L. Glashow, Phys. Lett 11, 255 (1964);
S.L. Glashow, J. Iliopoulos and L. Maiani, Phys. Rev. D2, 1285 (1970)

2. J.J. Aubert et al., Phys. Rev. Lett. 33, 1404 (1974);
J.E. Augustin et al., Phys. Rev. Lett. 33, 1406 (1974)

3. A. Benvenuti et al., Phys. Rev. Lett. 34, 419 (1975)
B.C. Barish et al., Colloq. Int. CNRS 245, 131 (1975)

4. W.F. Fry, Invited Paper KD2 at Spring Meeting, Washington, D.C. of APS, Bulletin of the American Physical Society 21, 679 (1976)

5. M.K. Gaillard, B.W. Lee and J.L. Rosner, Reviews of Modern Physics 47, 277 (1975)

6. H. Crannell et al., Phys. Rev. 7, 730 (1973)

7. J. Engler et al., Nucl Instr. and Meth. 106, 189 (1973)

8. PHS Consortium Data. D. Fong et al., Nucl.Phys. B102, 386 (1976) and private communication

9. J.V. Beaupre et al., Phys. Letters 37B, 432 (1971)

10. T.F. Kycia, Proceedings of the XVII International Conference on High Energy Physics, London (1974), pp. 1-32.

11. A.N. Diddens, Proceedings of the XVII International Conference on High Energy Physics, London (1974), pp. 1-41

12. D. Bogert et al., Phys. Rev. Letters 31, 1271 (1973)

13. D. Bogert et al., NAL-CGNF/SS-EXP (submitted to the XVII International Conference on High Energy Physics, London (1974)

14. For very long lifetimes ($\sim 10^{-12}$ sec) this reduction factor cannot be used. However, we can then require the observation of both D's which will reduce both strange and interaction backgrounds to negligible levels.

15. F. Villa, International Conference on Instrumentation for High Energy Physics, Frascati (1973)

16. σ_{diff} (20 atmos., 370 ns) $= \dfrac{100}{(800/370)} \times \dfrac{1}{\sqrt{(20/2.16)}} = 15\ \mu$

17. L.P. Kotenko et al., Nucl. Instr. and Meth. 54, 119 (1967)

18. E. Gygi and F. Schneider, p. 127 of Proceedings of the First International Conference on Streamer Chamber Technology, September 14-15, 1972, Argonne National Laboratory

19. F. Rohrbach, p. 161, International Conference on Instrumentation for High Energy Physics, Frascati (1973)

20. Cf. p. 725, Technique of Microwave Measurements, edited by C.G. Montgomery, M.I.T. Radiation Laboratory Series, Boston Technical Lithographics, Inc. (1963)

FIGURE CAPTIONS

1. Layout of the experiment showing beam defining scintillators S1, S2, VH1, the high pressure streamer chamber, the interaction hodoscope H, the hadron filter, the muon trigger scintillator S3, and the proportional (or drift) chambers P1, P2 which define the penetrating muon position ($\sim .5$ cm) and direction ($\sim .3^{o}$).

2. The high pressure streamer chamber assembly.

3. Computer simulation of a $D\bar{D}$ event (with additional pions) with two D particle decay tracks which miss the vertex. See Section III-C for further explanation.

4. The event of Fig. 3 with "eyeball" straight line fits drawn on the two decay tracks.

5. Scanning detection efficiency for $D\bar{D}$ events with central or peripheral production model. See Section III-C for further explanation.

6. Illustration of the scaling principle used in the high pressure streamer chamber design.

7. Layout of the spark gap and Blumlein geometry for the high pressure streamer chamber.

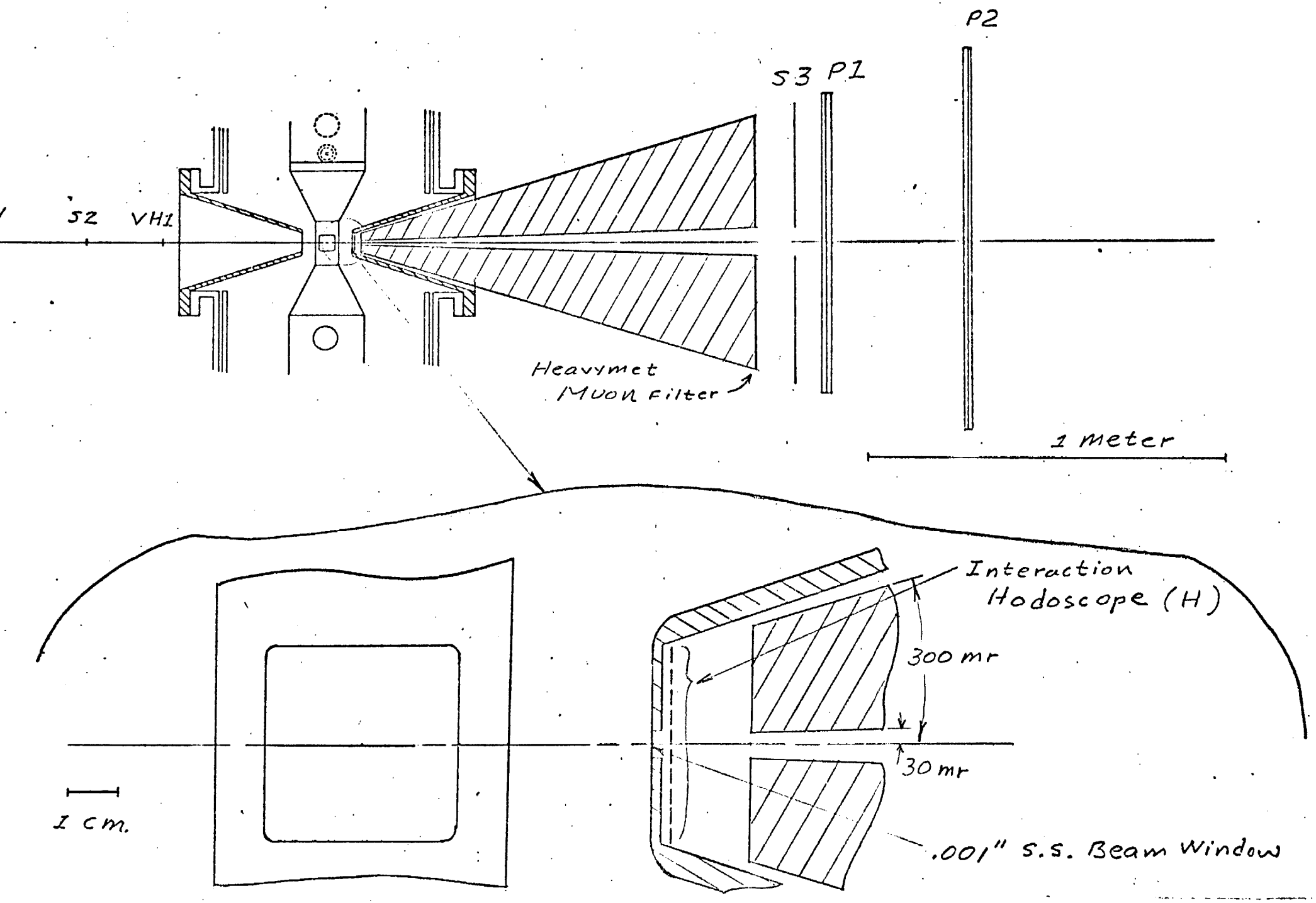
P2
S3
P1
S2
VH1
Heavymet
Muon Filter
1 meter
Interaction
Hodoscope (H)
300 mr
30 mr
1 cm.
.001" S.S. Beam Window

FIG. 1

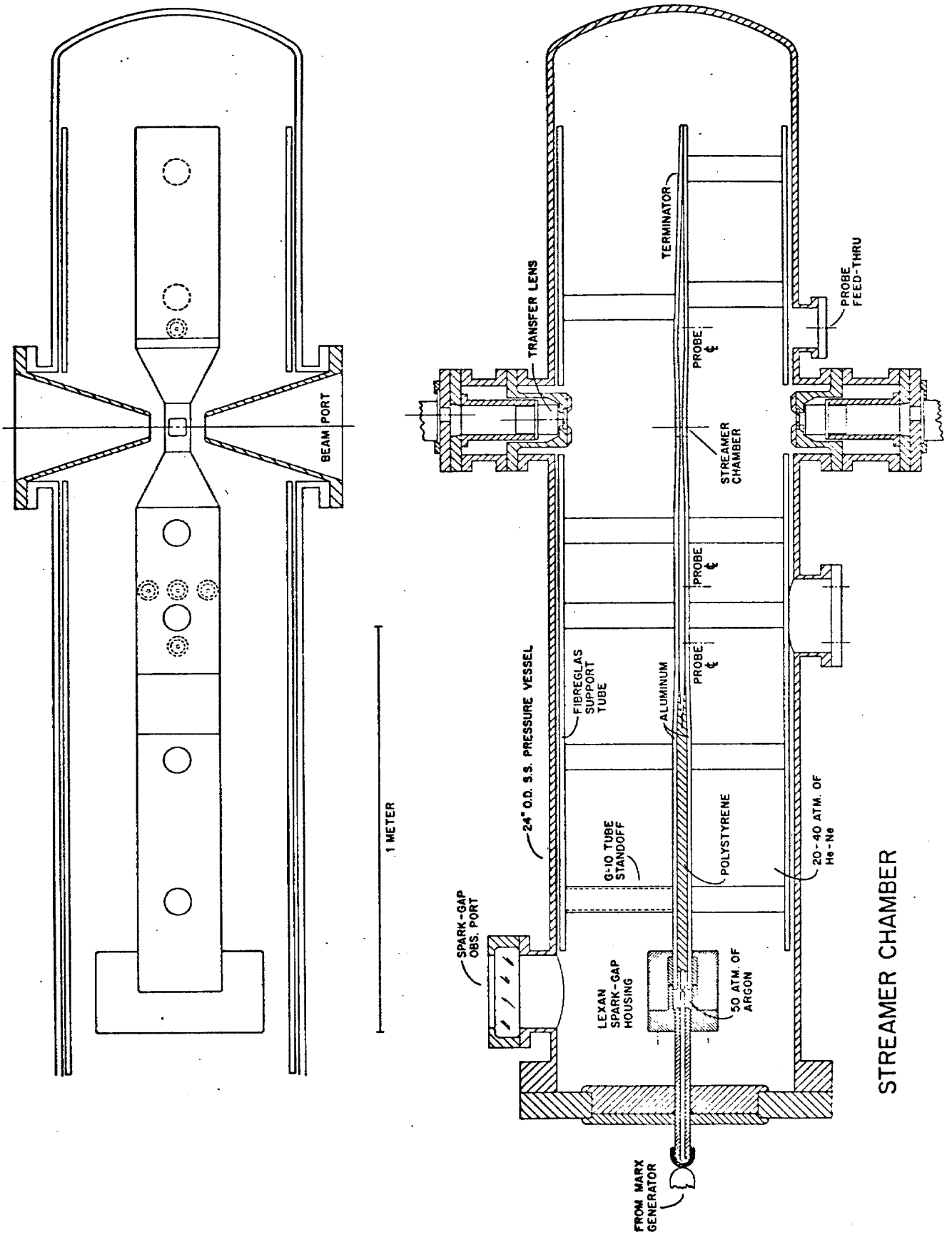

FIG. 2

STREAMER CHAMBER

490
(32)

FIG. 3

FIG. 4

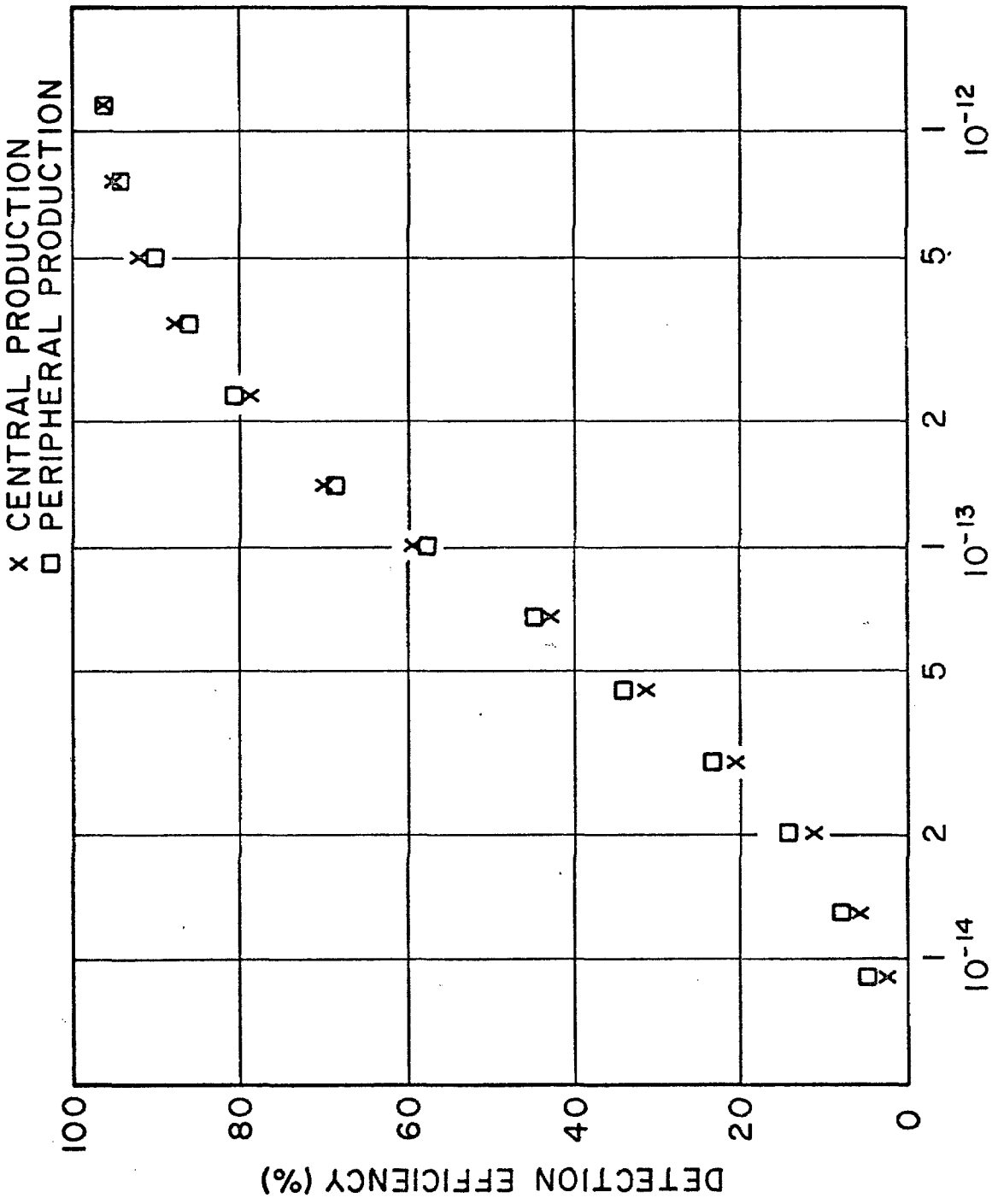
× CENTRAL PRODUCTION
□ PERIPHERAL PRODUCTION
DETECTION EFFICIENCY (%)
100
80
60
40
20
0
10^{-14}
2
5
10^{-13}
2
5
10^{-12}
t_0 in seconds

FIG. 5

Scaling Principle

raise pressure a factor S

raise electric field a factor S

reduce pulse duration a factor S

P_o, E_o, t_o $4P_o, 4E_o, t_o/4$

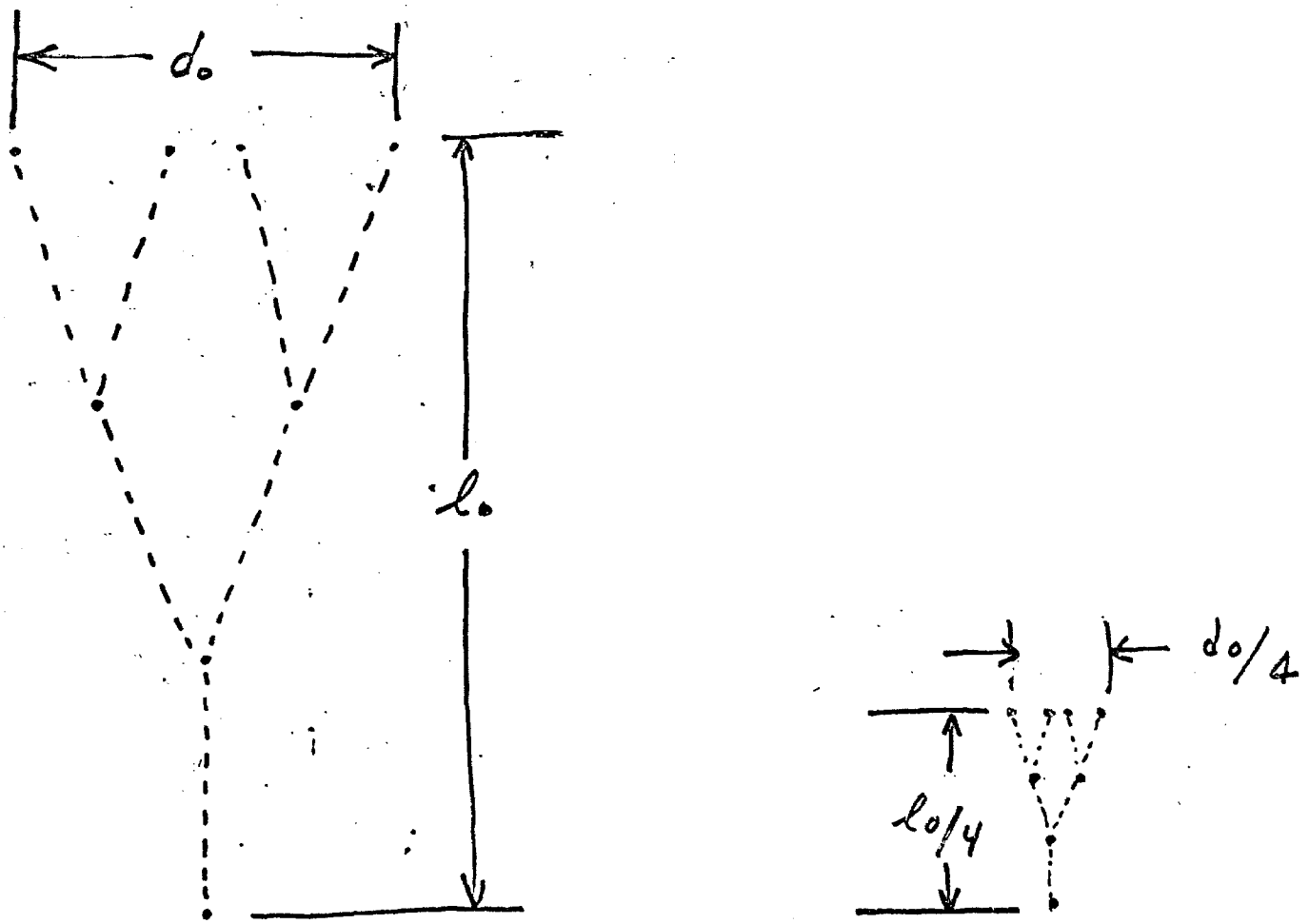

FIG. 6

Addendum to
Fermilab Proposal No. 490

Scientific Spokesman:

J. Sandweiss
Yale University
(203) 436-1581

SEARCH FOR SHORT LIVED PARTICLES USING A HIGH RESOLUTION STREAMER CHAMBER

T. Cardello, M. Dine, D. Ljung, T. Ludlam, R. Majka, L. Tzeng,
P. Nemethy, J. Sandweiss, A. Schiz, J. Slaughter, H. Taft

Yale University, New Haven, Connecticut 06520

M. Atac and S. Ecklund

Fermi National Accelerator Laboratory, Batavia, Illinois 60510

May 1977

A. General

Experiment 490 was first proposed in May 1976. Its goal is to use a high pressure, high resolution streamer chamber to study both the hadronic production and the subsequent decays of new short lived particles-presumably the charmed mesons and baryons, evidence for which has accumulated in experiments at SPEAR and Fermilab in the last few years.

With the expected resolution of 10 μm, we will be able to observe particles with lifetimes as short as 2.5×10^{-14} sec. The high density of the chamber gas which serves as the target, the use of an efficient trigger based on the semi-leptonic (muonic) decay of the new particles, and the 4π acceptance of the visual detection lead to a useful sensitivity to production cross sections comparable to the hadronic production cross sections for the ψ/J at Fermilab energies.

The experiment requires a floor space of approximately 2m x 3m and a 200 GeV/c π^- beam at an intensity of 8×10^5/spill. The original proposal requested 800 hours of data taking time in the beam.

Following the advice of the PAC, the laboratory approved the experiment for 600 hours of beam time conditional upon successful demonstration of chamber performance. In the past year we have constructed the chamber and currently have it under test at Yale. A report on the chamber test results will be separately presented; however, from the results to date we believe the chamber will

operate successfully at 40 atmospheres and have used this pressure in the rate estimates which are given below.

Although many small (but vital) details about "correct" chamber construction have been learned in the past year, the design of the chamber is essentially as given in the May 1976 proposal and in the interest of brevity is not repeated here. For reference, a drawing of the chamber system is given in Figure 1.

We have also carried out a careful study of the trigger system and of background rates using a set of Monte Carlo programs which use the best available information on high energy interactions and which can accurately simulate the physical disposition of the proposed experiment. Although the overall result is not significantly different from the more approximate estimates given in the May 1976 proposal, there are some important differences of detail and one fairly major addition of experimental equipment, the MWPC system imbedded in the hadron filter. The results of this study and redesign and a summary of the event and background rates are given in the following sections. Our capability to scan and measure the pictures and in particular to rapidly analyze the data is described in the last section.

B. Experiment Design

The final design is shown in Figure 2. The chamber is pulsed when a good beam track ($S1 \cdot S2 \cdot \overline{VH1}$) interacts in the chamber gas or thin windows, ($\Sigma H_i \geq 2$), and one or more particles penetrate the hadron filter (S3). The design of the hadron filter involves a trade-off

between hadron rejection and decay muon acceptance.

Most models for the hadronic production of the new particles lead to the expectation that they will be produced centrally with $X_{Feynman} \approx 0$. Data on the hadronic production of ψ/J support this view. Such central production leads to a rather low energy for the decay muon in the laboratory. For example half of the decay muons from X=0 D mesons would have lab energies below 5 GeV. Our design (optimized assuming various reasonable models of new particle production) has a minimum muon energy to trigger of ~3 GeV.

For such a "thin" hadron absorber, penetration by 2nd or 3rd generation hadrons tends to be more important than hadron to muon decay in flight, with subsequent penetration by the muon. For this reason one wants an absorber with the most hadron absorbtion lengths per unit (ionization) energy loss. Thus iron is the favored choice rather than heavymet, a fairly important practical change from the May 1976 proposal.

Detailed Monte Carlo calculations, taking the finite size of the beam (assumed to be 1 cm x 1 mm in cross section) into account led to the special shape of the central hole in the filter as shown in Figure 3.

Our best estimate of the "fake trigger" rate, i.e. the probability that an ordinary interaction will erroneously trigger the chamber is 0.3%. It is interesting to note that the best false rate which could be obtained with a heavymet absorber with the same minimum muon energy was about 2.5 times larger.

To estimate the trigger efficiency we have assumed that the new particles are produced with a rapidity spectrum

$$\frac{d\sigma}{dy} \propto e^{\frac{-y^2}{2}} + e^{-\frac{(y-1)^2}{2}}$$

and with $\frac{d\sigma}{dP^2} \propto e^{-1.5P^2}$. This choice of y distribution is motivated by our expectation of largely central production modified by a modest shift to $x>0$ due to the use of incident pions as suggested by ψ/J production. The trigger efficiency of 30% is not particularly sensitive to reasonable variations in these assumptions.

The major sources of background in the experiment are strange particle decays and secondary interactions. While these will not cause us to erroneously discover short lived particles (because their decay length distribution will be flat) they do establish a noise level which degrades the sensitivity of the experiment. We have found that these backgrounds can be reduced to nearly negligible levels by using a multiwire proportional chamber system imbedded in the hadron filter as shown in Figure 2. The properties of these chambers are given in Table I.

Table I

MWPC System in Hadron Filter

Chamber Cluster	Distance from Streamer Chamber Center (CM)	Number and Type of Planes	Chamber Dimensions (CM)	Wire Spacing (CM)
A	75	3(X,Y,U)	45x45	1
B	135	3(X,Y,V)	81x81	1
C	195	3(X,Y,U)	117x117	2
D	275	3(X,Y,V)	165x165	2

Total Number of Wires = 802

These chambers are used in two ways. First, the pattern of hits can be analyzed for consistency with the hypothesis that a penetrating particle was a muon produced in the primary interaction. Our Monte Carlo studies indicate that by this off line analysis we can, conservatively, reduce the number of fake triggers which must be scanned, by a factor of 2.5 while rejecting only 12% of the real, new particle, semi-leptonic decay events.

Secondly, we can apply the criterion that at least one of the tracks observed in the short lived event under study line up within suitable errors with the muon track detected and measured in the MWPC system. This requirement reduces background due to K^os by a factor of 16, due to Λ^o, Σ^o, $\Sigma^{\pm}$ by a factor of 32 and that due to secondary interactions by a factor of 8. Weighting these rejection factors according to the importance of the background type indicates an effective rejection of background events by a factor of 13.5. We estimate that 75% of the found real events will pass this test. Thus the MWPC system results in a net reduction of background by a factor of 2.5 x 13.5 = 34 while reducing the efficiency for real events to .88 x .75 = 66% of its previous value. The reduction of the scanning load by a factor of 2.5 will also be of considerable value in achieving rapid analysis of the data. For these reasons we believe the MWPC system to be an important addition to our earlier design.

Finally, we mention one further possible addition to the experiment - a muon range telescope which could provide a measure

of muon energy up to roughly 10 GeV. This would allow quite useful measurement of the muon transverse momentum in the new particle semi-leptonic decay. Such measurements might well turn out to be useful in disentangling decays due to several different new particle species. They would also be useful in relating the particles we find (hopefully!) to the charmed particles which have been studied via electromagnetic and weak production. We do not have at this time a detailed design and cost estimates nor do we know whether a suitable device already exists and could be borrowed.

C. Event Rates and Backgrounds

We have obtained new input data for our rate calculations from the detailed Monte Carlo simulation of the experiment (See section B). Here we give our revised results. We assume, for reference, a proper liftime, $\tau_0 = 10^{-13}$ sec and a muonic branching ratio, $B_\mu = 10\%$ for the short lived particles. For running time we use our approved 600 hours throughout this section.

With the chamber pressurized to 40 atm. the total interaction probability in the chamber gas and windows is $2.2\ 10^{-3}$ per incident pion. The level of false triggers (punchthroughs) in the muon detector is 0.3% per interaction. The trigger rate for the apparatus is therefore

$$R(\text{trigger}) = 6.7 \times 10^{-6}/\text{incident pion.}$$

With 8×10^5 pions/spill incident on the chamber, the event rate is 5.4/spill. A 37% camera deadtime leaves 3.4 live events/spill. We collect a total of 7.3×10^5 pictures, of which 24% have an interaction in the fiducial region:

$$N(\text{fiducial}) = 1.8 \times 10^5.$$

The number of "charmed $D\bar{D}$ events" in these photographs is proportional to $\sigma_D\ B_\mu\ \varepsilon_\mu$, where σ_D is the $D\bar{D}$ pair production cross section on nucleons, B_μ the muonic branching ratio, and $\varepsilon_\mu = 30\%$ is the efficiency of the muon detector for muons from D decay (Section B). We obtain for the total number of charmed decays

on film:

$$N(D\bar{D})/\sigma_D = 168 \text{ evt}/\mu b.$$

By requiring (off-line) a clean muon track in the proportional chambers of the muon filter we reduce the number of punchthroughs by a factor of 2.5, with an estimated 12% loss in muon detection efficiency.

The number of "good muon" pictures, which must be scanned, is therefore

$$N(SCAN) = 7.2 \times 10^4;$$

the number of charmed events in these pictures is

$$N_\mu(D\bar{D})/\sigma_D = 148 \text{ evt}/\mu b.$$

The scanning efficiency (at $t_o = 10^{-13}$) of 58% drops to 44% after we impose the requirement that the muon track in the muon detector be one of the identified tracks from the secondary vertex. The final number of identified charmed decays is thus

$$N(\text{detected } D\bar{D})/\sigma_D = 65 \text{ evt}/\mu b.$$

We note that this rate corresponds to a density of 1 charmed event/μb per 1100 scanned pictures.

Strange particle decays and secondary interactions are the dominant background in the experiment. We expect 225 strange decays and 173 interactions somewhere in the fiducial region;

41 of these occur in the first mm after the primary vertex, the region of interest for short-lived decays. The final requirement, that the muon line up with one of the observed D-decay products, reduces the background to 3.0 events. This background rate corresponds to a 45 nb level of $D\bar{D}$ production.

D. Scanning and Measuring

Approximately 1/4 of the total sample of pictures will have an interaction within the fiducial volume. The film will be scanned (in one view) to locate these events, and each track examined with sufficient accuracy to identify short-lifetime decay vertices with the efficiency discussed in our original proposal. This procedure will yield a small sample of candidate events which will then be subjected to further measurement, including measurement in the second view in order to determine whether one of the decay tracks lines up with the trajectory of the trigger muon.

At Yale we presently have two image plane digitizers operational with optics and film drive configured for the 35 mm film from the 30 inch hybrid bubble chamber facility at Fermilab. These are on-line to a DEC PDP-1 computer. The electronic, optical and most of the mechanical components for bringing up a third such machine are in hand, and we intend to have three such machines operating when the experiment begins. In terms of measurement precision and film-to-table magnification these machines are well

suited to the streamer chamber application.

It should be noted that the image size recorded on film by the 1.5:1 optics of our chamber is roughly the same as that recorded by the conventional large streamer chambers, or by the 30-inch bubble chamber, so that little modification of standard scanning and measuring techniques is required.

The task for automatic measuring devices is simplified by the fact that we are dealing here with straight-line tracks. At Yale we have a fully operational PEPR system which is currently measuring 30 inch bubble chamber film. We intend, at first, to employ PEPR for high precision measurements of our selected sample of candidate events for short-lifetime decays. As the experiment progresses we will investigate broader application of automatic measuring (and scanning) techniques to increase the rate of data reduction from the film.

We regard the rapid determination of the essential, first results of this experiment as a matter of critical importance. To this end we intend, as mentioned above, to have 3 IPD machines operational. We are prepared to staff these machines at two shifts per day. From our previous experience with similar event topologies in visual detectors (and our experience in scanning for Monte Carlo generated fake decays imbedded in real events from the 30-inch bubble chamber), we estimate the rate for scanning and measuring to be such that we will process 10 fiducial-volume interactions per machine-hour, for a total of approximately 10^4 fiducial-volume interactions per month. This is to be compared with the expected

7.2×10^4 such events with a "clean" muon trigger in the full data sample (see Sec. C). Thus our scanning and measuring capabilities will allow us to obtain preliminary results from a significant fraction of the full data sample within a month.

Figure Captions

Figure 1. The high resolution streamer chamber assembly.

Figure 2. Layout of the experiment showing beam defining scintillators S1, S2, VH1, the high pressure streamer chamber, the interaction hodoscope H, the hadron filter, the muon trigger scintillator S3, and the multiwire proportional chambers imbedded in the hadron filter.

Figure 3. Detail of the geometry of the hadron filter.

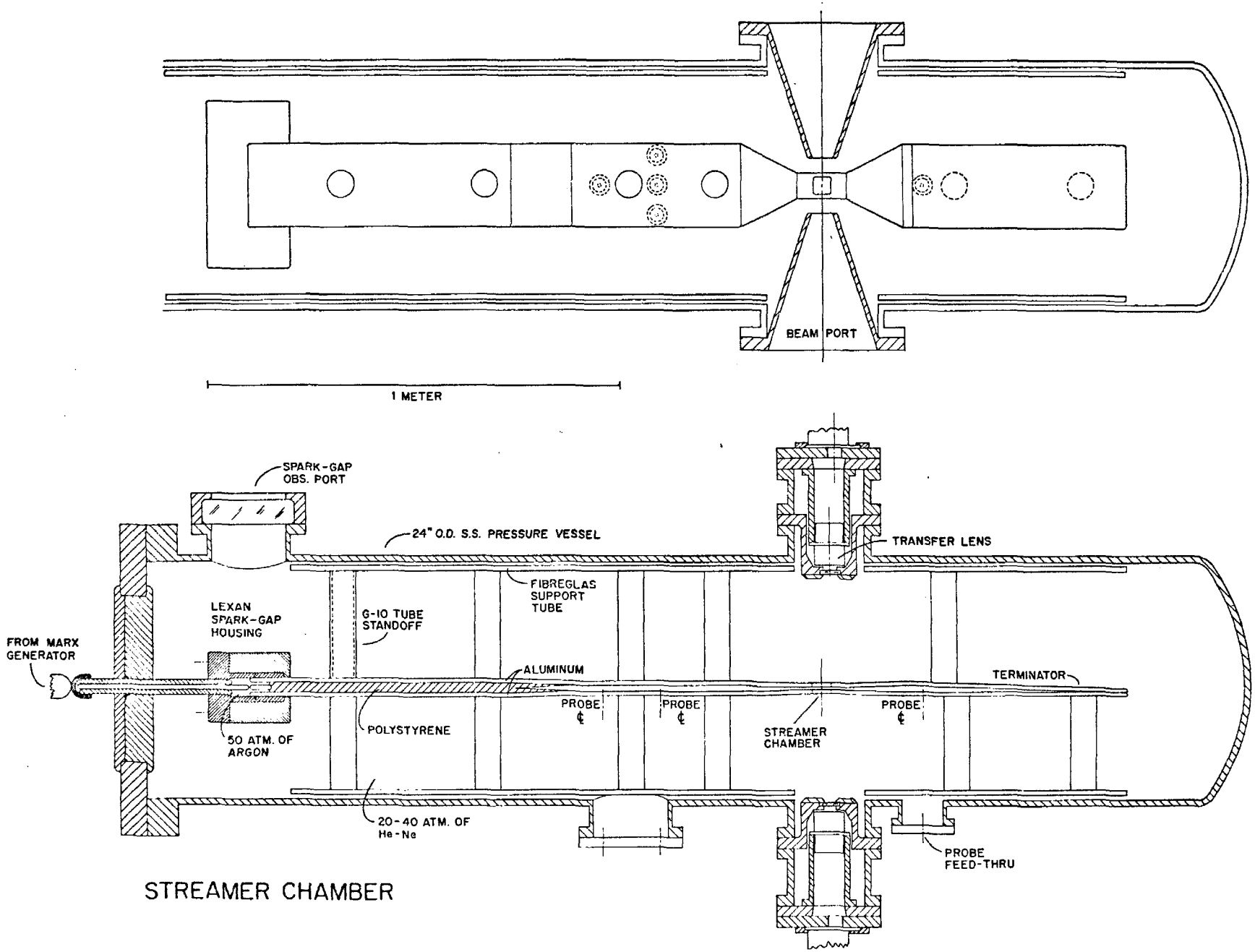
BEAM PORT
1 METER
SPARK-GAP OBS. PORT
24" O.D. S.S. PRESSURE VESSEL
TRANSFER LENS
FIBREGLAS SUPPORT TUBE
LEXAN SPARK-GAP HOUSING
G-10 TUBE STANDOFF
FROM MARX GENERATOR
ALUMINUM
TERMINATOR
PROBE ¢
PROBE ¢
PROBE ¢
STREAMER CHAMBER
50 ATM. OF ARGON
POLYSTYRENE
20-40 ATM. OF He-Ne
PROBE FEED-THRU
STREAMER CHAMBER

Fig. 1

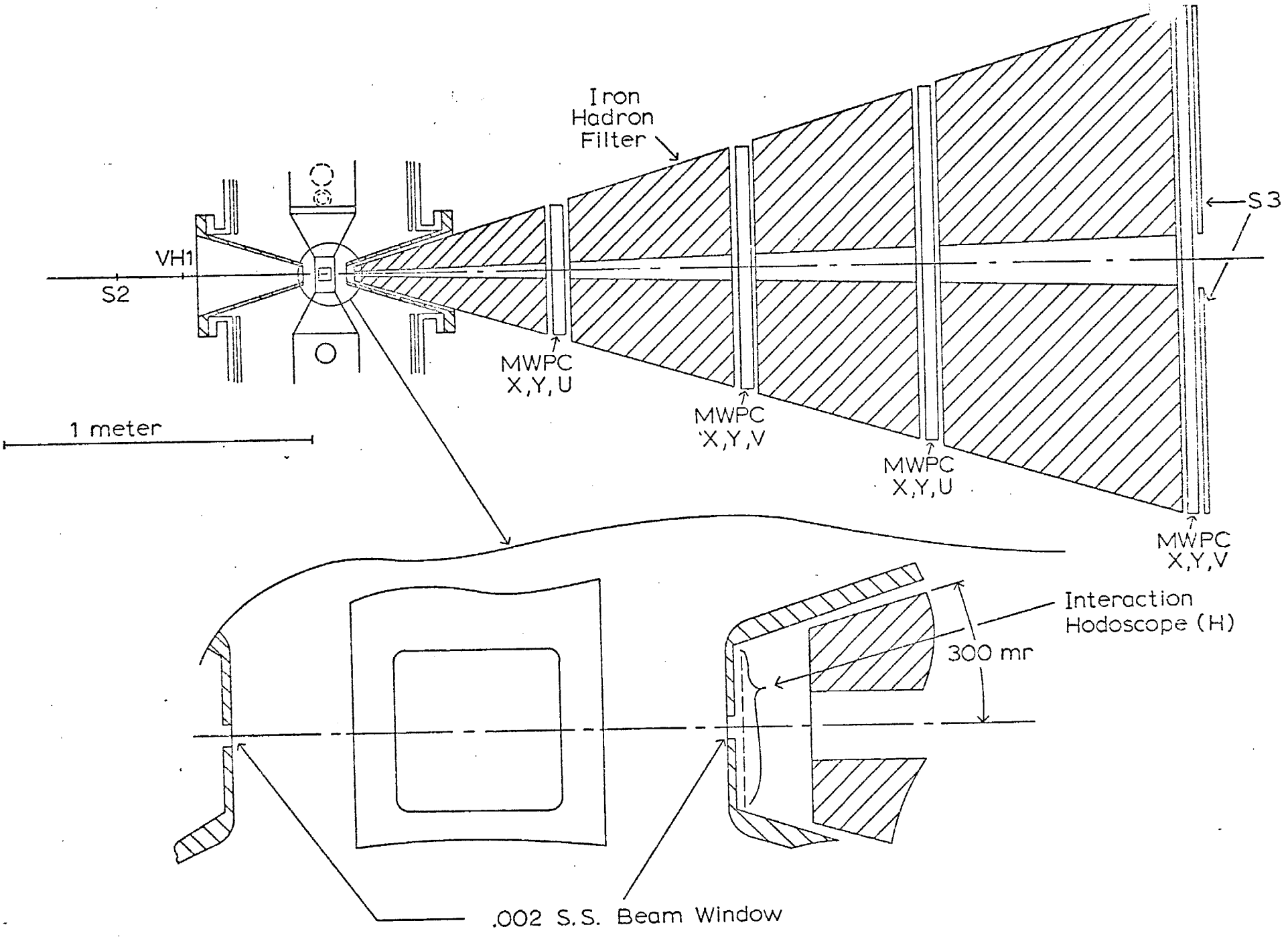
Iron
Hadron
Filter
S3
VH1
S2
MWPC
X,Y,U
MWPC
X,Y,V
MWPC
X,Y,U
MWPC
X,Y,V
1 meter
Interaction
Hodoscope (H)
300 mr
.002 S.S. Beam Window
1cm

Fig. 2

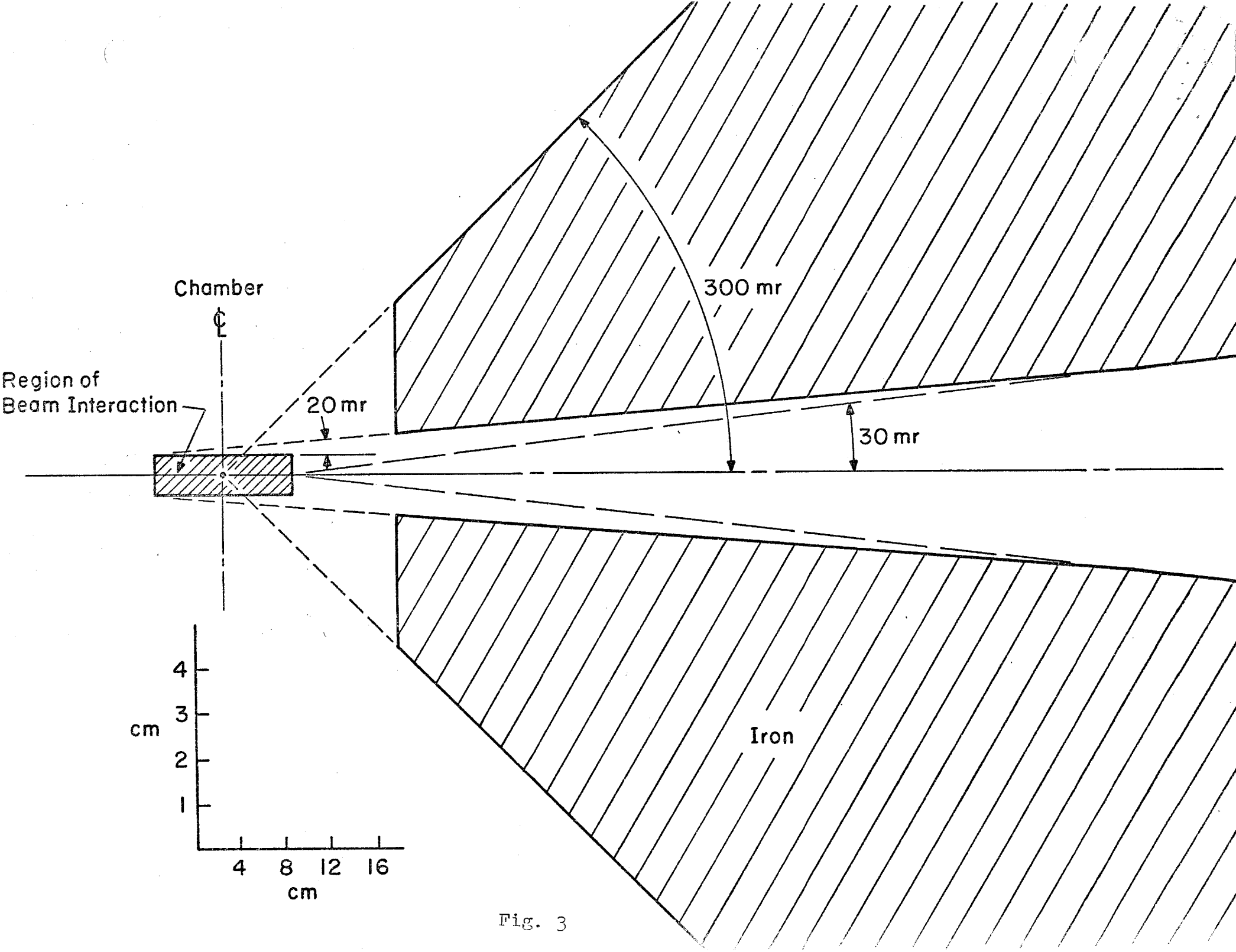
Chamber
℄
Region of
Beam Interaction
20 mr
300 mr
30 mr
Iron
cm
4
3
2
1
4
8
12
16
cm

Fig. 3